Enabling High Spectral Resolution of Liquid Mixtures in Porous Media by Anti-diagonal Projections of 2D ^{1}H NMR COSY Spectra

Camilla Terenzi[1,§], Andrew J. Sederman[1,], Michael D. Mantle[1], Lynn F. Gladden[1]*

[1]Department of Chemical Engineering and Biotechnology, University of Cambridge, Philippa Fawcett Drive, West Cambridge Site, Cambridge, CB3 0AS (UK)

AUTHOR INFORMATION

Corresponding Author

*Corresponding Author. E-mail: ajs40@cam.ac.uk

ABSTRACT. The non-invasive, *in situ* chemical identification of liquid mixtures confined in porous materials is experimentally challenging. NMR is chemically-resolved and applicable to optically-opaque systems, but suffers from a significant loss in spectral resolution in the presence of the magnetic field inhomogeneities typical of porous media. In this work, we introduce a method of analysis of conventional 2D ^{1}H NMR COSY spectra based on the extraction of 1D anti-diagonal projections, which are free from line-broadening effects and can therefore be used for chemical species identification. Here, we show the application of the technique to the measurement of linear *n*-alkanes where the cross-to-diagonal peak ratios are shown to follow a power-law curve as a function of the chain length. This calibration enables quantifying mixtures of linear hydrocarbons confined in any porous material independently of temperature or *inter*-molecular dynamics. Thus, this is a promising tool for quantitative chemical reaction monitoring studies in heterogeneous systems under *operando* experimental conditions.

TOC GRAPHICS

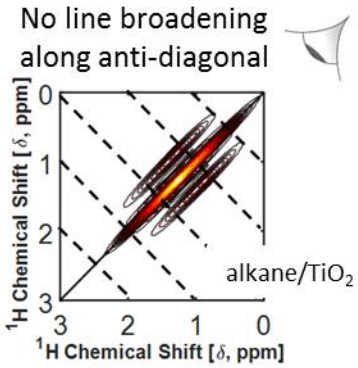

KEYWORDS. 2D NMR Spectroscopy, line broadening, magnetic susceptibility, porous media, hydrocarbons, chain length.

Quantifying the chemical composition of complex liquid mixtures within heterogeneous porous materials *in situ* under *operando* conditions of temperature and pressure is essential in many research areas, from oil and gas reaction engineering and catalysis, to biotechnology and the pharmaceutical industry. Yet, non-invasively identifying chemical species in real time remains a major challenge when liquids are confined in porous media, such as in catalyst particles. Optical spectroscopies such as confocal Raman [1–3], FT-IR [4,5], or UV [6,7] can be used to measure chemical concentrations at surfaces, but are difficult to use in multi-phase reactors, and will not provide measurements within the porous media. Neutron scattering [5,8,9] can provide a bulk measurement from liquids within a porous medium, but is mostly sensitive to physico-chemical interactions at liquid/solid interfaces, rather than to the chemical composition of the confined liquids themselves. Imbibed liquids are therefore mostly analyzed *ex situ* at ambient conditions, after their extraction from the porous material, e.g. by means of solvents or Soxhlet extraction procedures in the case of high-viscosity liquids [10]. Once the liquid is extracted, standard liquid-phase compositional analysis techniques such as mass spectrometry, liquid chromatography and near-infrared vibrational spectroscopy are typically used.

NMR is a potentially applicable technique as it is non-invasive, highly chemically-selective and applicable to optically-opaque liquid and/or solid materials. NMR is widely used for chemical species identification and is increasingly being used for reaction monitoring, often by means of low-field benchtop instrumentation [11–14]. However these measurements are usually done on single phase liquid samples because of the excessive spectral broadening that occurs in porous media. This spectral line broadening and subsequent loss of chemical resolution is due to the distortions in magnetic field that occur when materials of different magnetic susceptibility, such as a liquid in a porous medium, are placed inside the magnetic field. These distortions are

typically on the order of 1 ppm of the overall magnetic field which leads to a line broadening of ~1 ppm and is enough to loose chemical resolution in ^{1}H NMR spectra. Other techniques have been proposed to recover 1D and 2D NMR spectral resolution for liquid samples in the presence of heterogeneities in the static magnetic field [15–18]; however, these methods rely on deconvolution of reference peaks, and are not applicable in confined liquids where strong sample-dependent pore-scale magnetic field inhomogeneities are also present.

An example of the typical loss of spectral resolution from bulk to confined liquids is shown in Figure 1, where the 1D ^{1}H NMR spectrum of *n*-octane is shown both for pure bulk *n*-octane and *n*-octane imbibed in mesoporous TiO_2 pellets. Both spectra were acquired on a 300 MHz wide-bore Bruker Avance III HD spectrometer. The two main peaks of *n*-octane due to CH_2 (1.26 ppm) and CH_3 (0.88 ppm) groups are well resolved for the bulk *n*-octane sample, whilst only a single broad peak is observed for the *n*-octane imbibed in the porous TiO_2. The line-broadening observed for the *n*-octane in TiO_2 is due to the magnetic susceptibility difference between the liquid and solid phases which causes strong local variations in the magnetic field, or resonant frequency, and thus a wide spread in the measured ^{1}H chemical shift values.

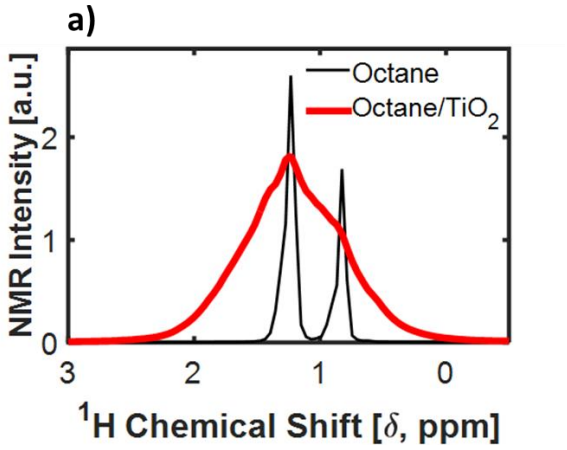

Figure 1. 1D ^{1}H NMR spectrum of bulk liquid *n*-octane (thin black line) and of liquid *n*-octane imbibed in TiO_2 pellets (thick red line). The latter intensity, arising solely from *intra*-particle liquid, has been magnified × 16.

In this work, we introduce a method for performing peak analysis of conventional 2D ^{1}H NMR COrrelation SpectroscopY (COSY) [19,20] spectra of multi-spin liquid systems, which removes the effect of line broadening due to pore-scale magnetic susceptibility effects. This is achieved by analyzing the 2D COSY peaks in a 1D sub-spectrum created by summing the 2D signals along the anti-diagonal direction: the result is a 1D spectral projection perpendicular to the main COSY diagonal. Using bulk and confined linear hydrocarbons as test systems, we show that (i) spectral resolution is retained in these anti-diagonal projections despite the presence of magnetic field inhomogeneities, and that (ii) our method can be used to quantify the mean chain length of confined mixtures of linear *n*-alkanes independent of system-specific variables, such as temperature and *inter*-molecular dynamics. 2D COSY spectra are a powerful analytical tool for chemical structure elucidation in small molecules, due to their ability to trace out *intra*-molecular J-coupling networks [19,20]. In a standard COSY measurement of a bulk liquid system, two non-equivalent protons H_A and H_B connected by up to three chemical bonds, with non-null coupling J_{AB} and non-null chemical shift difference, $\Delta\delta_{AB} = \delta_A - \delta_B$, undergo magnetization transfer which causes splitting of the on-diagonal intensities into a pair of symmetric cross-peaks at (δ_A, δ_B) and (δ_B, δ_A) located on either side of the main diagonal [19,20]. Provided that $|\Delta\delta_{AB}| \gg |J_{AB}| \gg 0$, such cross-peaks are well resolved and contain *intra*-molecular chemical information that is not provided by 1D spectra. This is shown in Figure 2a, where the COSY spectrum of liquid *n*-octane shows two well-resolved on-diagonal peaks at 1.26 ppm and 0.88 ppm,

respectively corresponding to the CH_2 and CH_3 signals seen in Figure 1. The off-diagonal cross-peaks at (1.26 ppm, 0.88 ppm) and (0.88 ppm, 1.26 ppm) arise from CH_2-CH_3 magnetization transfer, specifically via the three-bond ${}^3J$-coupling ($\sim$ 7 Hz) between each CH_3 group and the outmost CH_2 group directly attached to it [21]. We note that (i) the four-bond ${}^4J$-coupling interaction between each CH_3 group and the second-nearest CH_2 group in the alkane chain is practically zero ($\sim$ - 0.07 Hz), thus yielding negligible cross-peak intensities, and that (ii) the overlapping CH_2 signals give rise to poorly resolved cross-peaks in spite of their non-negligible ${}^3J$-coupling ($\sim$ 6.8 Hz) [21]. Figure 2b shows two 1D anti-diagonal projections from samples of *n*-alkanes of different carbon number (*n*-octane and *n*-hexadecane) obtained over the ^{1}H chemical shift range of [- 4 ppm: 7 ppm] from the respective COSY measurements. The x-axis of the anti-diagonal projections, after being scaled by a factor of $\sqrt{2}$ and having its zero-value set to the position of the total on-diagonal peak, represents the ^{1}H chemical shift difference, here denoted $\Delta\delta$, between signals in the 1D spectrum that give rise to the paired satellite cross-peaks. For example in the case of linear alkanes, $\Delta\delta = \pm$ 0.38 ppm corresponds to the chemical shift difference between the J-coupled CH_3 and CH_2 moieties at 1.26 ppm and 0.88 ppm (see Figure 1). The peaks in this anti-diagonal projection can be analyzed to give quantitative chemical information. Calculation of *n*-alkane carbon number can be made by comparing the total area of the paired symmetric cross-peaks, I^{XP}, to that of the on-diagonal peaks, I^{diag}, as it is only the interaction between the CH_3 and its adjacent CH_2 that contribute to the cross peaks at $\Delta\delta$ = 0.38 ppm. The intensity of these peaks acts as a measure of the concentration of CH_3-CH_2 moieties in the sample. Hence, taking the I^{XP}/I^{diag} ratio provides a measure of the chain length, in which sample-dependent relaxation effects cancel out. Moreover,

such measurement is independent of sample environment parameters, such as temperature and pressure, as well as strength and homogeneity of the applied static magnetic field.

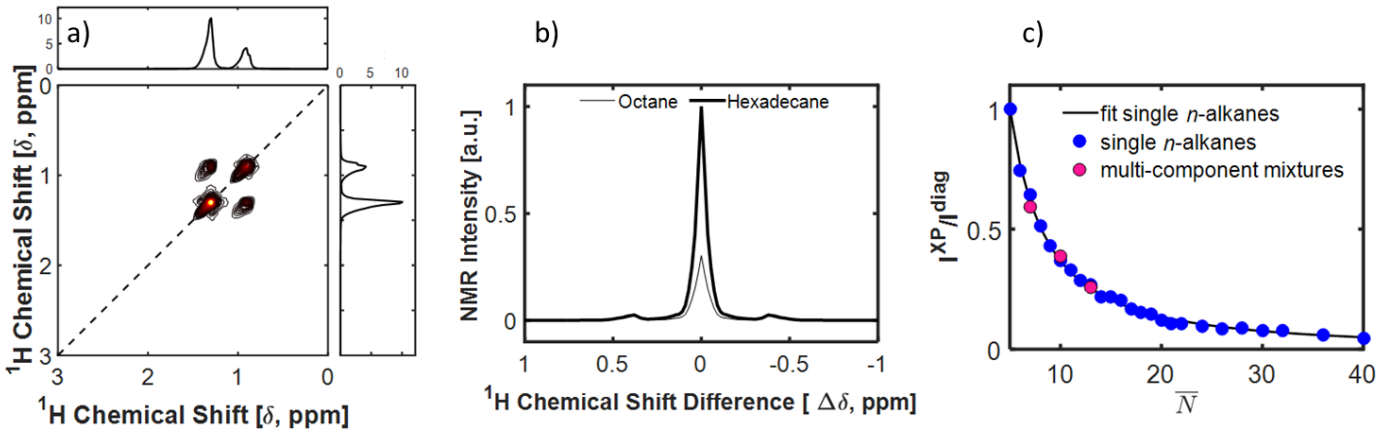

Figure 2 a) 2D ^{1}H NMR COSY spectrum of bulk *n*-octane. b) Anti-diagonal projection of the 2D COSY spectrum for bulk *n*-octane (thin line) and bulk *n*-hexadecane (thick line). c) Cross-to-diagonal intensity ratios, I^{XP}/I^{diag}, for single (blue circles) and multi-component mixtures (pink circles) of bulk *n*-alkanes as a function of the average chain length $\overline{N}$ and normalized to the I^{XP}/I^{diag} ratio of *n*-pentane. The solid line is the Levenberg-Marquardt fit to the power-law function $I^{XP}/I^{diag}(\overline{N}) = a \cdot (\overline{N})^{-b}$, with $a = 10.2 \pm 0.7$ and $b = 1.44 \pm 0.04$.

Figure 2c shows how this technique can be used to quantitatively measure the average chain length, $\overline{N}$, of single component *n*-alkane samples and of mixtures of *n*-alkanes. In Figure 2c, the I^{XP}/I^{diag} values for bulk linear alkanes are plotted for a range of N up to *n*-tetracontane ($N = 40$) normalized to the I^{XP}/I^{diag} ratio of liquid *n*-pentane. Samples with $N > 16$, which are not in liquid state at room temperature, were measured at temperatures within the range 40 °C and 160 °C depending on their melting point (see Experimental). The fit shown in Figure 2c demonstrates that the I^{XP}/I^{diag} ratios accurately follow a power-law decay. A similar power-

law behavior is also observed for NMR spin relaxation rates or self-diffusion coefficients in linear n-alkanes [22–24]; however, this COSY approach is independent of assumptions on *inter*-molecular dynamics and, thus, can be generalized to the analysis of bulk or confined mixtures at any temperature and pressure without assumptions about molecular motion. This generalized approach is applicable to multi-component liquid mixtures for quantifying the mean chain length, here indicated as $\bar{N}$. To demonstrate this, COSY measurements were performed on three liquid mixtures with gravimetric estimates of $\bar{N}$ = 7, 9.4 and 13 (see Experimental), obtained as Gaussian molar distributions of single-component linear alkanes in the liquid range at room temperature ($5 < N \leq 16$). These data are also plotted in Figure 2c, and the NMR-estimates of $\bar{N}$ obtained by using the same curve as that used for the single liquids were calculated to be 7.2 ± 0.7, 9.7 ± 0.8 and 12.8 ± 1.4, all in excellent agreement with the gravimetric measurement and within the experimental error obtained from the fit.

In Figure 3 we demonstrate the applicability of this analysis for calculating $\bar{N}$ in single-components or mixtures of linear *n*-alkanes confined in porous media. Figure 3a shows the COSY spectrum of liquid *n*-octane imbibed in TiO_2 porous pellets: significant line-broadening occurs parallel to the main diagonal, thus making the usual volume integration of COSY cross-peaks unfeasible in contrast to the result shown for bulk *n*-octane in Figure 2a; however, no significant broadening is seen perpendicular to the main diagonal. This is because the cross peaks in the COSY spectra are due to a purely *intra*-molecular, J-coupling, spin interaction, and the distance of each cross peak from the diagonal is defined only by the *intra*-molecular chemical-shift difference between the J-coupled spins. Even in the presence of pore- or sample-scale magnetic field inhomogeneities, the local magnetic field difference remains uniform at the sub-molecular length scale of the J-coupling spin interaction. Therefore, whilst the local

magnetic field and susceptibility does alter the position of a peak along the diagonal, as in 1D NMR spectroscopy measurements, the distance of each cross peak from the diagonal is unaffected. For this reason, spectral broadening does not occur perpendicular to the main COSY diagonal and enables spectral resolution to be retained. Figure 3b confirms this, where the 1D anti-diagonal summed projection spectrum for *n*-octane and *n*-hexadecane imbibed in TiO_2 is seen to be very similar to the projection of the bulk 2D COSY spectrum (Figure 2b), and there is clear spectral separation of the on-diagonal intensity from the cross peaks.

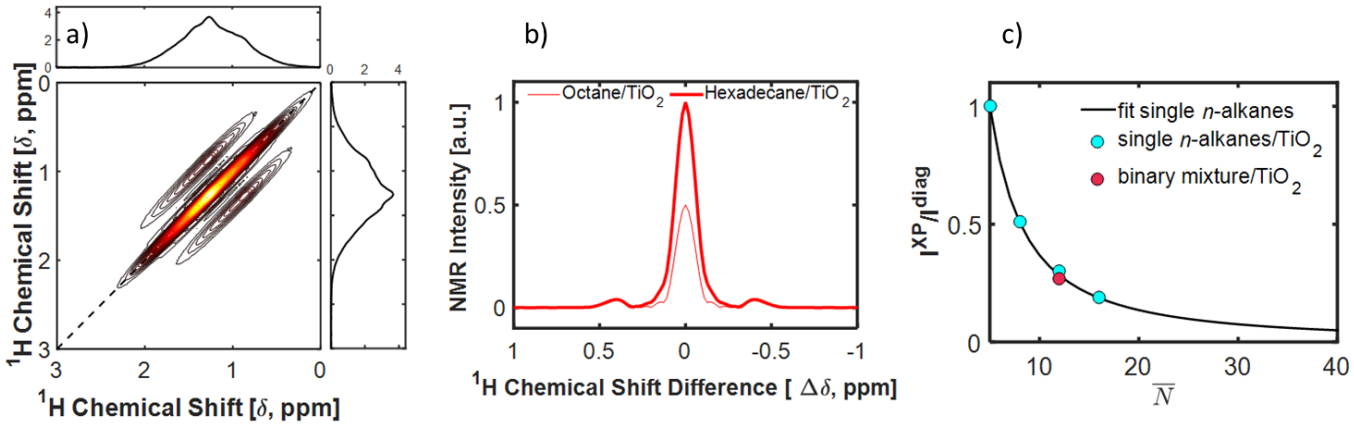

Figure 3 a) 2D ^{1}H NMR COSY spectrum of *n*-octane imbibed in TiO_2 pellets. b) Anti-diagonal projection of the 2D COSY spectrum for *n*-octane (thin line) and *n*-hexadecane (thick line) imbibed in TiO_2. c) I^{XP}/I^{diag} for *n*-pentane, *n*-octane, *n*-dodecane and *n*-hexadecane (cyan circles), and for a 48:52 mol% binary mixture of *n*-octane/*n*-hexadecane (dark pink circles), all normalized to the I^{XP}/I^{diag} ratio of *n*-pentane/TiO_2 sample and compared with the fitting curve in Figure 2c.

Figure 3c shows the experimentally determined I^{XP}/I^{diag} ratios for a range of pure linear alkanes (pentane, octane, dodecane and hexadecane) confined in TiO_2 pellets and a binary *n*-octane/*n*-hexadecane mixture (48:52 mol%, $\bar{N} = 12.2$) confined in TiO_2 pellets, along with the same calibration curve used in Figure 2c for pure bulk liquids. Data in Figure 3c are normalized to the I^{XP}/I^{diag} ratio of *n*-pentane in TiO_2. The data show excellent agreement to the power-law calibration curve, and that the local environment of the liquid in the porous media does not have a significant effect on the I^{XP}/I^{diag} ratio. Using the power-law model, the recovered $\bar{N}$, is equal to 8.4 ± 0.8, 12.5 ± 1.4 and 16 ± 2 for *n*-octane, *n*-dodecane and *n*-hexadecane respectively, and to 12.4 ± 1.4 for the mixture, in excellent agreement with the nominal or gravimetrically calculated values. In this application we have used linear alkane chains and assumed that the mixture is made up of exclusively *n*-alkanes, but the presence of branching could also be identified by the appearance of other peaks. In particular, coupling between CH_3 and CH would become significant and peaks would be apparent at the appropriate $\Delta\delta$ between the CH_3 and CH peaks. However, in order to quantify the amount and type of branching that was present, it is likely that further calibration experiments would be needed.

We conclude that the proposed method for COSY cross-peaks integration is effective for the chemical analysis of complex liquids in porous media where high spectral resolution, lost in 1D NMR spectroscopy, is recovered in the COSY anti-diagonal spectral projection.

In spite of an emerging interest in real-time industrial applications of 2D NMR spectroscopy, involving the use of compressed-sensing [25], ultra-fast single-scan acquisitions with benchtop instrumentation[13], or solid-state magic angle spinning (MAS) measurements[26,27] , the feasibility of such approaches for chemical structure elucidation in heterogeneous liquid/solid systems is limited because of spectral line broadening. Our approach for resolving cross-peaks

along the anti-diagonal direction in conventional COSY spectra is applicable in the presence of severe line broadening at any static magnetic field and in any porous material, without the need for spectral deconvolution procedures or system-dependent model assumptions.

We thus envisage immediate applications of our proposed method for *in situ* monitoring of chemical/biochemical reactions[13,14,27–30] under real experimental conditions, e.g. under flow of complex multi-component liquids at *operando* temperature and pressures, as well as in the chemical characterization of liquid mixtures inside rigid and soft multi-component systems.

Experimental

Materials: Linear *n*-alkanes in the range of chain length from pentane to hexadecane were purchased from Sigma-Aldrich; higher linear *n*-alkanes ($16 < N \leq 40$) were purchased from Fischer Scientific (99% Alfa Aesar™ or 98% ACROS Organics™). All liquids were used as received. The TiO_2 porous catalyst pellets were provided by Shell Global Solutions International B.V. and had nominal pore size of 26 ± 4 nm.

Three bulk liquid samples with different multi-component Gaussian molar distributions were prepared from single-component linear alkanes with $N \leq 16$, within the liquid range at room temperature. The molar percentages used for the three samples were: (i) $N = 5$ (6.7%), 6 (23%), 7 (40%), 8 (24%), 9 (6.1%); (ii) $N = 7$ (2.6%), 8 (13%), 9 (37%), 10 (44%), 11 (3.2%); and (iii) $N = 10$ (1.3%), 12 (48%), 14 (49%), 16 (1.3%). The respective molar-weighted $\bar{N}$ values for samples (i), (ii) and (iii) were thus 7, 9.4 and 13.

For each liquid-imbibed porous sample, the TiO_2 pellets were dried (105 °C, 12h) and then soaked in liquids overnight; the excess liquid was then wiped off taking care of not

removing the *intra*-particle liquid. Each sample was transferred to a 5 mm sealed NMR tube before measurements.

All NMR data were acquired at 300 MHz on Bruker Avance spectrometers using 5 mm diameter NMR sample tubes. For $N > 16$ an extended variable temperature RF coil, equipped with temperature control unit and rated up to 200˚C, was used where the measurement temperature was fixed at a value within the range 40-160 °C depending on the melting point of the alkane. 2D ^{1}H NMR spectra using a conventional gradient-COSY pulse sequence (*cosygpqf* in Topspin, Bruker) were acquired using 2048 x 256 points in the direct and indirect dimensions, respectively, over a spectral width of 5500 Hz. The signal was summed over two acquisitions separated by a recycle time of 1 s, resulting in about 10 mins measurement time. Measurements were repeated at least twice in the above conditions. Further repeats at increased recycle times of 10 s confirmed that recycle time had no effect on the peak ratios calculated. COSY Spectra were Fourier-transformed, symmetrized and baseline-corrected in Topspin. Further data analysis, including the calculation of anti-diagonal spectral projections, was performed in MATLAB.

AUTHOR INFORMATION

* Corresponding author. E-mail: ajs40@cam.ac.uk

§ Current Address. Camilla Terenzi1: Laboratory of Biophysics, Wageningen University and Research, Stippeneng 4, 6708 WE, Wageningen (The Netherlands)

Notes

The authors declare no competing financial interests.

Acknowledgment

The authors thank Shell Global Solutions International B.V. for funding, and for providing the TiO_2 porous catalyst support and its pore-size characterization.

REFERENCES

(1) Rank, D. H.; Scott, R. W.; Fenske, M. R. Qualitative and Quantitative Analysis of Hydrocarbon Mixtures by Means of Their Raman Spectra. *Ind. Eng. Chem. Anal. Ed.* **1942**, *14*, 816–819.

(2) Hou, M.; Huang, Y.; Ma, L.; Zhang, Z. Compositional Analysis of Ternary and Binary Chemical Mixtures by Surface-Enhanced Raman Scattering at Trace Levels. *Nanoscale Res. Lett.* **2015**, *10*, 1–7.

(3) Andrews, A. B.; Wang, D.; Marzec, K. M.; Mullins, O. C.; Crozier, K. B. Surface Enhanced Raman Spectroscopy of Polycyclic Aromatic Hydrocarbons and Molecular Asphaltenes. *Chem. Phys. Lett.* **2015**, *620*, 139–143.

(4) Jentoft, F. C.; Kröhnert, J.; Subbotina, I. R.; Kazansky, V. B. Quantitative Analysis of IR Intensities of Alkanes Adsorbed on Solid Acid Catalysts. *J. Phys. Chem. C* **2013**, *117*, 5873–5881.

(5) Shimomura, T.; Inoue, S.; Kadohata, S.; Umecky, T.; Takamuku, T. SANS, ATR-IR, and 1D- and 2D-NMR Studies of Mixing States of Imidazolium-Based Ionic Liquid and Aryl Solvents. *Phys. Chem. Chem. Phys.* **2013**, *15*, 20565–20576.

(6) Harrell, M. L.; Malinski, T.; Torres-López, C.; Gonzalez, K.; Suriboot, J.; Bergbreiter, D. E. Alternatives for Conventional Alkane Solvents. *J. Am. Chem. Soc.* **2016**, *138*, 14650–14657.

(7) Jones, R. N. The Ultraviolet Absorption Spectra of Aromatic Hydrocarbons. *Chem. Rev.* **1943**, *32*, 1–46.

(8) Székely, N. K.; Almásy, L.; Rădulescu, A.; Rosta, L. Small-Angle Neutron Scattering Study of Aqueous Solutions of Pentanediol and Hexanediol. In *J. Appl. Crystallogr.*; 2007; Vol. 40, pp 307–311.

(9) Sastry, N. V.; Vaghela, N. M.; Aswal, V. K. Effect of Alkyl Chain Length and Head Group on Surface Active and Aggregation Behavior of Ionic Liquids in Water. *Fluid Phase Equilib.* **2012**, *327*, 22–29.

(10) Readman, J. W. Chemical Analysis of Hydrocarbons in Petroleum Oils and the Assessment of Environmental Contamination. In *Handbook of Hydrocarbon and Lipid Microbiology*; Springer Berlin Heidelberg: Berlin, Heidelberg, 2010; pp 3573–3582.

(11) Mitchell, J.; Gladden, L. F.; Chandrasekera, T. C.; Fordham, E. J. Low-Field Permanent Magnets for Industrial Process and Quality Control. *Prog. Nucl. Magn. Reson. Spectrosc.* **2014**, *76*, 1–60.

(12) Dalitz, F.; Cudaj, M.; Maiwald, M.; Guthausen, G. Process and Reaction Monitoring by

Low-Field NMR Spectroscopy. *Prog. Nucl. Magn. Reson. Spectrosc.* **2012**, *60*, 52–70.

(13) Gouilleux, B.; Charrier, B.; Danieli, E.; Dumez, J.-N.; Akoka, S.; Felpin, F.-X.; Rodriguez-Zubiri, M.; Giraudeau, P. Real-Time Reaction Monitoring by Ultrafast 2D NMR on a Benchtop Spectrometer. *Analyst* **2015**, *140*, 7854–7858.

(14) Singh, K.; Blümich, B. Desktop NMR for Structure Elucidation and Identification of Strychnine Adulteration. *Analyst* **2017**, *142*, 1459–1470.

(15) Sheberstov, K. F.; Sinitsyn, D. O.; Cheshkov, D. A.; Jeannerat, D. Elimination of Signals Tilting Caused by B_0 Field Inhomogeneity Using 2D-Lineshape Reference Deconvolution. *J. Magn. Reson.* **2017**, *281*, 229–240.

(16) Morris, G. A.; Barjat, H.; Horne, T. J. Reference Deconvolution Methods. *Prog. Nucl. Magn. Reson. Spectrosc.* **1997**, *31*, 197–257.

(17) Barjat, H.; Morris, G. A.; Swanson, A. G.; Smart, S.; Williams, S. C. R. Reference Deconvolution Using Multiplet Reference Signals. *J. Magn. Reson. Ser. A* **1995**, *116*, 206–214.

(18) Chen, Z.; Cai, S.; Huang, Y.; Lin, Y. High-Resolution NMR Spectroscopy in Inhomogeneous Fields. *Prog. Nucl. Magn. Reson. Spectrosc.* **2015**, *90–91*, 1–31.

(19) Keeler, J. *Understanding NMR Spectroscopy*; John Wiley & Sons: Chichester, 2010.

(20) Ernst, R.; Bodenhausen, G.; Wokaun, A. *Principles of Nuclear Magnetic Resonance in One and Two Dimensions*; Clarendon Press: Oxford, 1987.

(21) Tynkkynen, T.; Hassinen, T.; Tiainen, M.; Soininen, P.; Laatikainen, R. ^{1}H NMR Spectral Analysis and Conformational Behavior of N-Alkanes in Different Chemical Environments. *Magn. Reson. Chem.* **2012**, *50*, 598–607.

(22) Freed, D. E.; Burcaw, L.; Song, Y. Q. Scaling Laws for Diffusion Coefficients in Mixtures of Alkanes. *Phys. Rev. Lett.* **2005**, *94*.

(23) Meerwall, E. von; Beckman, S.; Jang, J.; Mattice, W. L. Diffusion of Liquid N-Alkanes: Free-Volume and Density Effects. *J. Chem. Phys.* **1998**, *108*, 4299.

(24) Freed, D. E. Dependence on Chain Length of NMR Relaxation Times in Mixtures of Alkanes. *J. Chem. Phys.* **2007**, *126*, 174502.

(25) Wu, Y.; D'Agostino, C.; Holland, D. J.; Gladden, L. F. In Situ Study of Reaction Kinetics Using Compressed Sensing NMR. *Chem. Commun.* **2014**, *50*, 14137–14140.

(26) Ashbrook, S. E.; Dawson, D. M.; Seymour, V. R. Recent Developments in Solid-State NMR Spectroscopy of Crystalline Microporous Materials. *Phys. Chem. Chem. Phys.* **2014**, *16*, 8223–8242.

(27) Hamdoun, G.; Gouilleux, B.; Sebban, M.; Barozzino-Consiglio, G.; Harrison-Marchand, A.; Giraudeau, P.; Maddaluno, J.; Oulyadi, H. 2D 7 Li Ultrafast CT-COSY: A New Tool for the Rapid Measurement of Tiny Homonuclear Lithium Scalar Couplings. *Chem. Commun.* **2017**, *53*, 220–223.

(28) Koda, M.; Furihata, K.; Wei, F.; Miyakawa, T.; Tanokura, M. F2-Selective Two-Dimensional NMR Spectroscopy for the Analysis of Minor Components in Foods. *Magn. Reson. Chem.* **2011**, *49*, 710–716.

(29) Sans, V.; Porwol, L.; Dragone, V.; Cronin, L. A Self Optimizing Synthetic Organic Reactor System Using Real-Time In-Line NMR Spectroscopy. *Chem. Sci.* **2015**, *6*, 1258–1264.

(30) Guennec, A. Le; Giraudeau, P.; Caldarelli, S.; Dumez, J.-N. Ultrafast Double-Quantum NMR Spectroscopy. *Chem. Commun.* **2015**, *51*, 354–357.